Available online at www.sciencedirect.com
SCIENCE DIRECT®
Journal of Magnetic Resonance 174 (2005) 325–330
JMR Journal of Magnetic Resonance
www.elsevier.com/locate/jmr

Communication

Correspondence between spin-dynamic phases and pulse program phases of NMR spectrometers

Michael H.A. Roehrl *, Gregory J. Heffron, Gerhard Wagner *

Department of Biological Chemistry and Molecular Pharmacology, Harvard Medical School, Boston, MA 02445, USA

Received 22 December 2004; revised 1 February 2005
Available online 3 March 2005

Abstract

Spin state selective experiments have become very useful tools in solution NMR spectroscopy, particularly in the context of TROSY line narrowing. However, the practical implementation of such pulse sequences is frequently complicated by unexpected instrument behavior. Furthermore, a literal theoretical analysis of sequences published with specific phase settings can fail to rationalize such experiments and can seemingly contradict experimental findings. In this communication, we develop a practical approach to this ostensible paradox. Spin-dynamic design, rationalization, and simulation of NMR pulse sequences, as well as their confident and reliable implementation across current spectrometer hardware platforms, require precise understanding of the underlying nutation axis conventions. While currently often approached empirically, we demonstrate with a simple but general pulse program how to uncover these correspondences a priori in the general case. From this, we deduce a correspondence table between the spin-dynamic phases used in NMR theory and simulation on the one hand and pulse program phases of current commercial spectrometers on the other. As a practical application of these results, we analyze implementations of the original ^{1}H–^{15}N TROSY experiment and illustrate how steady-state magnetization can be predictably, rather than empirically, added to a desired component. We show why and under which circumstances a literal adoption of phases from published sequences can lead to incorrect results. We suggest that pulse sequences should be consistently given with spin-dynamically correct (physical) phases, rather than in spectrometer-specific (software) syntax.

Keywords: Spin dynamics; Pulse/receiver phases; Spin state selective experiments; Pulse program implementation; Hardware differences

1. Introduction

NMR spectroscopy is a powerful method for the sophisticated manipulation of nuclear spin quantum states. In particular, spin state selective (S^3) experiments such as TROSY have proven to be particularly valuable in biomolecular liquid state NMR spectroscopy [1]. Another interesting area are recently proposed spin state selective heteronuclear *J* cross polarization experiments [2,3]. A third, even simpler example is the correct choice of pulse phases during an initial ^{1}H–^{15}N INEPT transfer to specifically add non-transferred steady-state ^{15}N magnetization to the desired TROSY component, rather than to subtract it [4–6]. All of these experiments entail the highly specific manipulation of spin states, and generally great care must be taken with the correct spin state assignment of spectral lines [7]. The experiments necessitate precise and predictable control of nutation axis phases in the rotating frame for spin-dynamic design, rationalization, and simulation of pulse sequences and, equally important, for their confident and reliable implementation across current spectrometer hardware platforms.

Inspired by a recent analysis of the potentially convoluted and confusing relationship between spin-dynamic

* Corresponding authors. Fax: +1 617 432 4383.
E-mail addresses: michael_roehrl@hms.harvard.edu (M.H.A. Roehrl), gerhard_wagner@hms.harvard.edu (G. Wagner).

1090-7807/$ - see front matter © 2005 Elsevier Inc. All rights reserved.
doi:10.1016/j.jmr.2005.02.001

phases as used in the theoretical treatment of NMR experiments and the phase nomenclature used for pulse programming of spectrometers [7,8], we analyzed these relationships for the most commonly used commercial biomolecular NMR instruments. Furthermore, we provide a prescription for how these relationships can be generally uncovered through a very simple NMR experiment. Our analysis relates in an explicit look-up table spin-dynamic (physical) phases as used in theory and simulation with (software) phases as they need to be specified within the framework of the pulse programming software of the spectrometer. We illustrate our findings with a detailed analysis of the pulse and receiver phases of the original, now classic ^{1}H–^{15}N TROSY experiment [1]. It will become apparent that a "naïve" correspondence, as might be deduced from software syntax, is not generally valid and can be misleading. This point is easily obfuscated in current instrument documentation. While the experienced pulse programmer will undoubtedly have encountered (and empirically accounted for) these practical intricacies before [4,5], we believe that a systematic presentation, including correspondence tables, and a general experimental verification procedure replace doubt with certainty and will benefit both the aspiring and advanced pulse sequence designer/programmer.

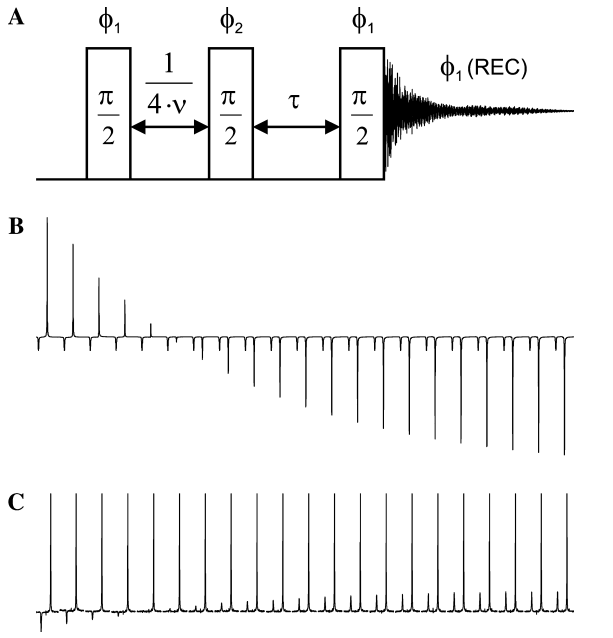

Fig. 1. (A) Pulse sequence for the determination of the correspondence between spin-dynamic and pulse program phases [7]. (B) Proton spectra acquired on a Bruker Avance DRX 500, demonstrating inversion recovery behavior of the more shielded resonance. (C) Proton spectra acquired on a Varian INOVA 500, demonstrating inversion recovery behavior of the less shielded resonance. See text for details.

2. Methods

Throughout, we define spin-dynamic phase behavior as one that uses rigorously both the signed vectorial relationship $\vec{\omega}_0 = -\gamma \cdot \vec{B}_0$ and the right-handed convention for all rotations and coordinate systems [6,9]. In all experiments, we employed our pulse calibration samples containing 0.1 M [^{13}C]methanol, 0.1 M [^{15}N]urea, and 10 mM DSS in DMSO-d_6, supplemented with 0.1 mg/ml Gd(III)Cl_3 for ^{1}H detection only. Direct ^{1}H, ^{13}C, and ^{15}N detection experiments were carried out at 298 K on our Bruker Avance DRX 500, DRX 600, AV 500, and AV 750 instruments (all using XWIN-NMR 3.5) and our Varian Mercury 200 (^{1}H and ^{13}C only) and INOVA 500 and 600 instruments (all using VNMR 6.1C).

3. Results and discussion

Fig. 1A illustrates a simple experiment, based on an earlier proposal by Levitt [7], that uncovers the relationship between spin-dynamic phase and pulse program phase on a spectrometer. We first discuss the behavior of spins with positive gyromagnetic ratio ($\gamma > 0$, such as ^{1}H, ^{13}C, and ^{31}P). With the spin-dynamic phase settings $\phi_1 = +x$ and $\phi_2 = +y$, a not coupled spin in initial state $+z$ that is ν hertz *less* shielded than the carrier position (i.e., to its left in a conventionally plotted spectrum) will be rotated back to $+z$ after the second $\pi/2$ pulse. Conversely, a spin that is ν hertz more shielded than the carrier position (i.e., to its right) will be inverted to $-z$. For nuclei with $\gamma < 0$ (e.g., ^{15}N), the result is the exact opposite, i.e., the less shielded spin will be rotated to $-z$, whereas the more shielded spin will return to $+z$. The third $\pi/2$ pulse after the variable delay τ serves as a read pulse to distinguish between the two possible outcomes, $+z$ and $-z$, since only the $-z$ state will display inversion recovery behavior as a function of τ (and thus T_1 relaxation), whereas the signal originating from $+z$ will be invariant with respect to τ.

Fig. 1B shows 21 successive ^{1}H spectra of two resonances with a chemical shift difference of 0.52 ppm. The spectra were acquired on a Bruker DRX 500 instrument with τ ranging from 0 ms (left) to 1 s (right) in increments of 50 ms and with a recycle delay of 5 s. The more shielded resonance corresponds to DSS, the less shielded smaller resonance corresponds to a minor contaminant in commercial grade DSS. Each resonance is not coupled. The carrier was set to the exact center between the two resonances, and ν was set equal to the distance in hertz between the carrier and the resonances. The same phase correction was applied throughout. ϕ_1 and ϕ_2 were "naïvely" programmed as "0" and "1," respectively. In agreement with spin-dynamic theory, only the more shielded DSS resonance experiences

Table 1
Correspondence between spin-dynamic pulse phases and pulse program phase syntax on our current Bruker and Varian spectrometers

Spin-dynamic nutation axis	Pulse program phase syntax			
	Bruker		Varian	
	$\gamma > 0$ (^{1}H, ^{13}C)	$\gamma < 0$ (^{15}N)	$\gamma > 0$ (^{1}H, ^{13}C)	$\gamma < 0$ (^{15}N)
$+x$	0	0	zero	zero
+y	1	**3**	**three**	one
$-x$	2	2	two	two
$-y$	3	**1**	**one**	three

The phases 0, 1, 2, 3, and zero, one, two, three correspond to 0°, 90°, 180°, and 270° in Bruker and Varian software syntax, respectively. On Varian, the observe phase has a numerical value rather than a keyword. Results are invariant with respect to cyclic pulse program phase permutations along the Bruker and Varian columns. The Bruker spectrometers tested at our site were Avance DRX 500/600 and AV 500/750, the Varian spectrometers tested were Mercury 200 and INOVA 500/600. Important differences are shown bold and underlined.

longitudinal relaxation with $T_1 \approx 330$ ms. Spin-dynamic and "naïve" pulse program phases are identical in this case (see Table 1).

Fig. 1C depicts 21 successive ^{1}H spectra acquired on a Varian INOVA 500 instrument using the same sample and acquisition parameters as in Fig. 1B. ϕ_1 and ϕ_2 were "naïvely" programmed as "zero" and "one," respectively. Here, the less shielded resonance experiences longitudinal relaxation ($T_1 \approx 330$ ms), indicating that spin-dynamic and "naïve" pulse program phases are not corresponding. The correct behavior would, for example, have been obtained by programming ϕ_1 and ϕ_2 as "zero" and "three," respectively (see Table 1).

Analogous experiments for ^{13}C and ^{15}N were carried out by directly observing the respective resonance and setting the carrier position either ν hertz above or below.

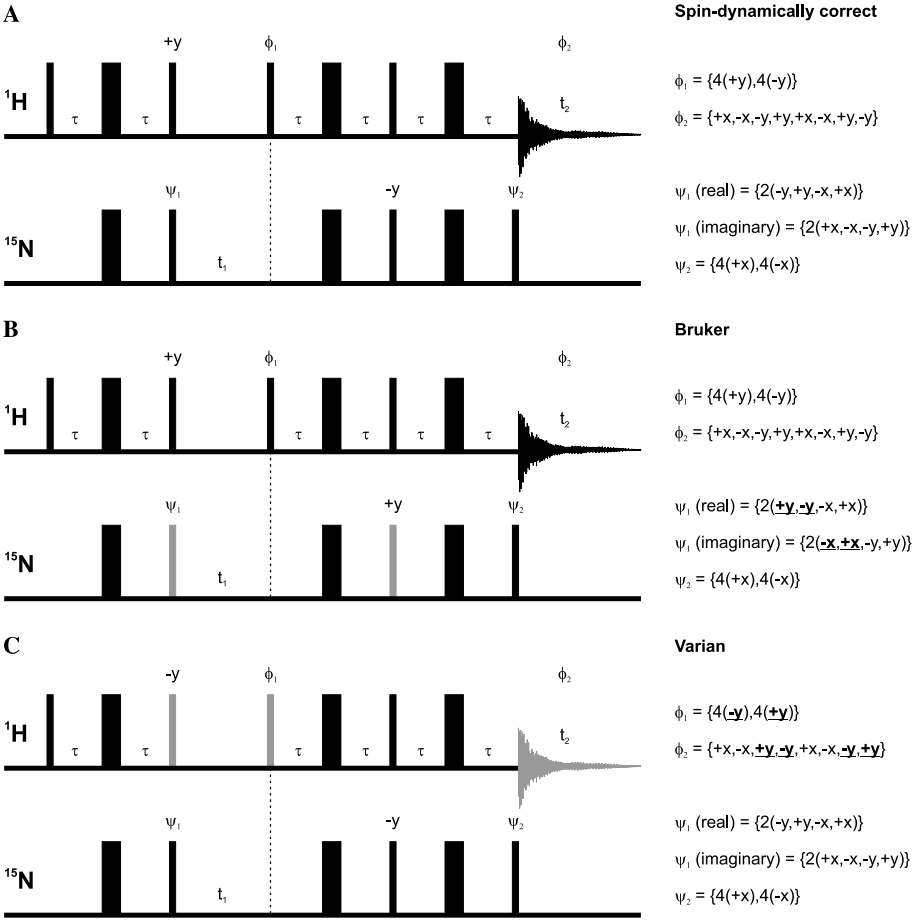

Fig. 2. ^{1}H–^{15}N TROSY–HSQC pulse sequences. (A) Spin-dynamically correct phase settings (see text). (B) Bruker software pulse program phase settings [1]. (C) Varian software pulse program phase settings. Differences from (A) are shown in grey or bold and underlined.

The results are summarized in Table 1. It provides a look-up table that describes the correspondence between spin-dynamic phase and pulse program software syntax for our Bruker and Varian spectrometers. The results show that the spectrometers at our site are mirror images with respect to their pulse program phase implementation. Bruker phase changes are right-handed for ^{1}H and ^{13}C but left-handed for ^{15}N, whereas Varian phase changes are left-handed for ^{1}H and ^{13}C but right-handed for ^{15}N. We find that it is the Varian phase behavior that coincides with an earlier analysis [7].

It is interesting to note that we did not detect the magnitudes of an instrument's Larmor frequencies as a potentially additional complicating factor [8], when comparing the behavior of proton and carbon on our low-field Varian Mercury 200 with that on higher-field INOVA instruments. A likely reason is that one consistent hardware frequency generation scheme is employed throughout.

To the best of our knowledge, the relationships in Table 1 hold for currently manufactured high-field instruments. However, since it is impossible to predict all potential combinations of hardware and software currently available, as well as taking into account the possibility of future changes by manufacturers or the introduction of new NMR spectrometers, we would like to caution readers from automatically adopting the results of Table 1 to their situation, but rather we recommend that spectroscopists use an experiment such as shown in Fig. 1A to explicitly determine the pulse program phase behavior of relevant nuclei. A similar recommendation has also been given previously [7,8].

As a practical application of our findings, we analyzed the original description of the ^{1}H–^{15}N TROSY experiment [1]. Fig. 2 depicts the TROSY pulse program with (A) spin-dynamically correct phase settings, (B) pulse program phase settings appropriate for Bruker spectrometers [1], and (C) pulse program phase settings appropriate for Varian spectrometers. It should be noted that the original publication provides the Bruker pulse program phase syntax, not spin-dynamically consistent phases. As a direct consequence, one cannot theoretically rationalize the experiment based on the phases

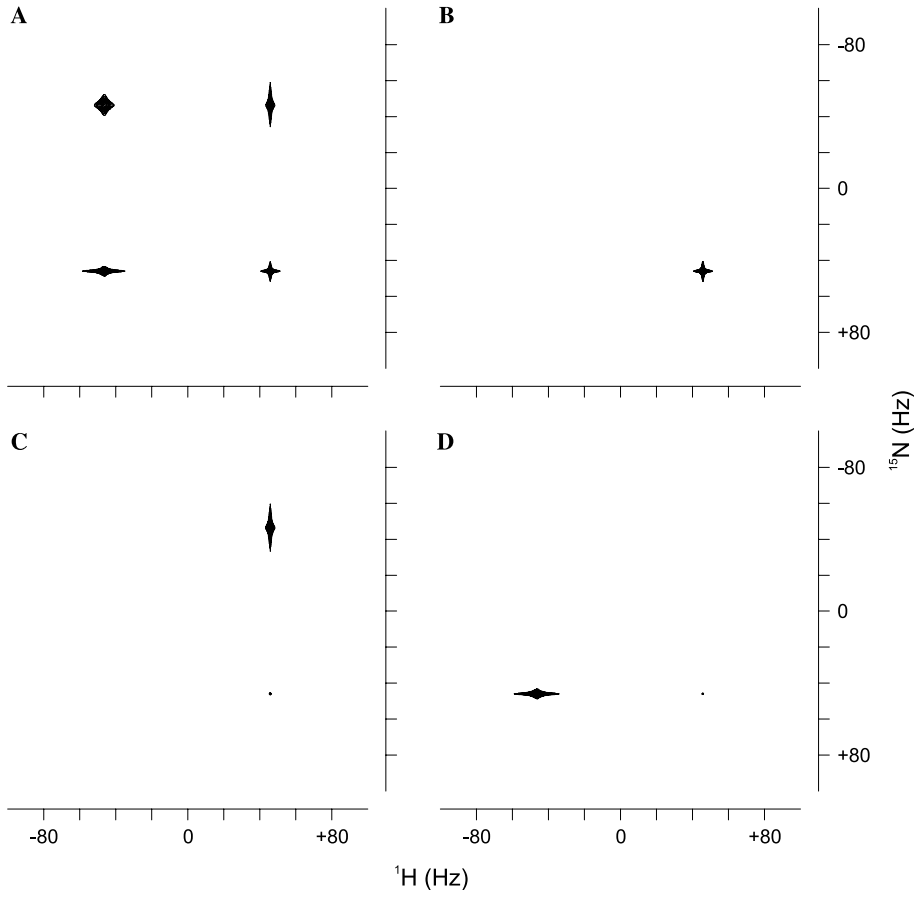

Fig. 3. Simulations of spectra of an isolated ^{1}H–^{15}N spin system. See text for detailed parameters. (A) Fully coupled HSQC. (B) TROSY spectrum with spin-dynamically correct phase settings (Fig. 2A). (C) TROSY spectrum with literally interpreted Bruker phase settings (Fig. 2B). (D) TROSY spectrum with literally interpreted Varian phase settings (Fig. 2C). In (B), the desired TROSY component is selected, while in (C) and (D) semi-TROSY components are erroneously selected.

given in Fig. 2B (vide infra), and, furthermore, an unaltered (i.e., literal) implementation on a Varian spectrometer would fail to correctly select the narrow TROSY component. Based on our introductory results (vide supra), it is readily seen that the phases given in Figs. 2B and C are related to those in Fig. 2A via the correspondences listed in Table 1 (differences are shown in grey or bold and underlined).

To illustrate the potential effects of "naïve" pulse program implementation, we simulated the three pulse sequences of Fig. 2, interpreting in every case the given phases literally as spin-dynamic phases. All simulations were carried out with the program QSim, which adopts rigorously the same spin-dynamic conventions that are used in this paper [10]. States-type spectra of an isolated ^{1}H–^{15}N spin pair were calculated with 512 complex points and spectral widths of 200 Hz in each dimension. A magnetic field strength of 14.09 T was assumed. Further parameters were $J_{NH} = -92$ Hz, $r_{NH} = 1.02$ Å, and $\tau = 2.72$ ms. The RF-field strengths of ^{1}H and ^{15}N pulses were set to 25 kHz. Both nuclei were chosen to be on resonance with the carriers (0 Hz offset). Lipari–Szabo relaxation parameters were set to $\tau_m = 5$ ns, $\tau_e = 50$ ps, and $S^2 = 0.8$. The axially symmetric chemical shielding anisotropies, $\sigma_{||}$–$\sigma_{\perp}$, were assumed to be +14 ppm (^{1}H) and −160 ppm (^{15}N), with associated angles between the unique tensor axes and the internuclear vector of 0° and 22°, respectively [11,12]. Please note that there exists sometimes confusion over the absolute signs of these anisotropies because different scales may be used, i.e., σ (shielding) or δ (shift). All spectra were processed identically using a squared sine window function, phased to give positive absorptive lines, and plotted such that deshielded proton and nitrogen frequencies are negative and positive, respectively [6]. Fig. 3A depicts a fully coupled HSQC spectrum for reference. As expected, the narrow TROSY component appears at $\Delta\omega(^{1}H) = +46$ Hz and $\Delta\omega(^{15}N) = +46$ Hz. Furthermore, two semi-TROSY peaks and one anti-TROSY peak are visible. Simulation of the spin-dynamically correct pulse sequence (Fig. 2A) yields the spectrum of Fig. 3B, illustrating the correct selection of the TROSY component. However, simulation of literally interpreted Bruker (Fig. 2B) or Varian (Fig. 2C) phase syntax demonstrates the selection of incorrect semi-TROSY components (Figs. 3C and D). This result reiterates the fact that the spectrometers use inconsistent phase conventions, since the pulse sequences of Figs. 2B and C do indeed work correctly on their respective platforms.

A further example is the implementation of an initial INEPT transfer step such that the preexisting steady-state magnetization of the receiving nucleus is added to the desired line (Fig. 4). Currently, this is often achieved by trial and error variation of INEPT pulse phases during experimental set-up. Our results allow a rational approach to this problem because we can predictably relate pulse program syntax with spin-dynamic considerations. Fig. 4A depicts an X-detected ^{1}H-X INEPT step, in which the final proton pulse phase is variable. Figs. 4B and C show antiphase spectra of [^{13}C]methanol and [^{15}N]urea in which steady-state magnetization adds to or subtracts from individual spectral lines (dashed lines), respectively. Note that the results for [^{13}C]methanol and [^{15}N]urea are similar because of $\gamma_C > 0$, $J_{HC} > 0$, and $\gamma_N < 0$, $J_{HN} < 0$ [6]. In the case of the ^{1}H–^{15}N INEPT (Fig. 4C), lines associated with a β

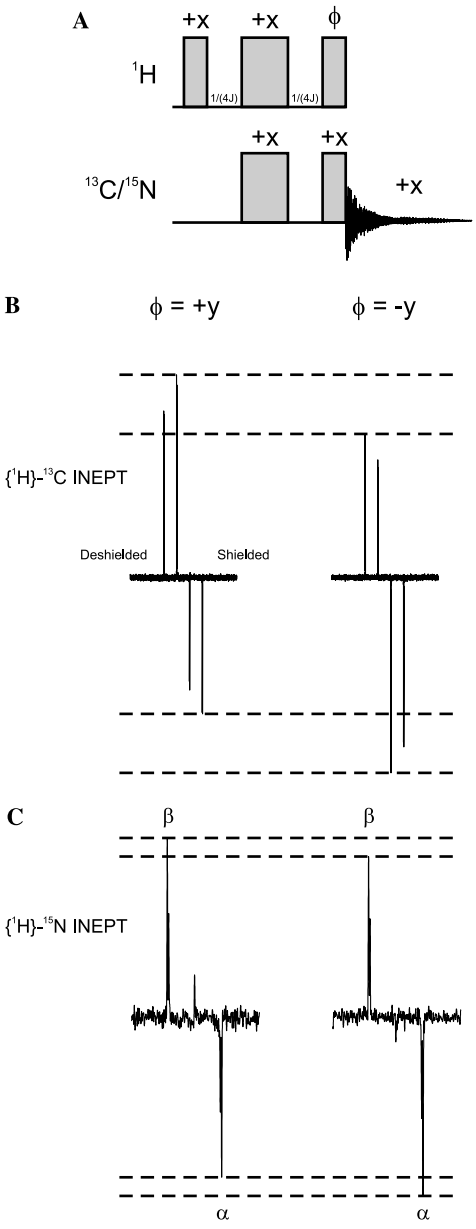

Fig. 4. INEPT experiments demonstrating the role of pulse phase settings for the selective addition/subtraction of steady-state magnetization to/from antiphase components. (A) Pulse sequence scheme with variable pulse phase ϕ. (B) {^{1}H}–^{13}C INEPT using [^{13}C]methanol. (C) {^{1}H}–^{15}N INEPT using [^{15}N]urea. All pulse phases are given spin-dynamically (see Table 1). Note that actual pulse program implementations may thus read differently [13].

state amide proton (left spectrum with $\phi = +y$; usually desirable in TROSY spectra) or an α state amide proton (right spectrum with $\phi = -y$) are enhanced, respectively. For example, the case $\phi = +y$ can be understood as follows: just prior to acquisition, the (larger) transferred magnetization is positively proportional to $+2I_zS_y$ ($\gamma_H > 0$), whereas the (smaller) steady-state component on ^{15}N is positively proportional to $-S_y$ ($\gamma_N < 0$). Expressing the two terms by their spin matrices, we have

$$+2I_zS_y = \frac{1}{2i}\begin{pmatrix} 0 & -1 & 0 & 0 \\ +1 & 0 & 0 & 0 \\ 0 & 0 & 0 & +1 \\ 0 & 0 & -1 & 0 \end{pmatrix}$$

and

$$-S_y = \frac{1}{2i}\begin{pmatrix} 0 & +1 & 0 & 0 \\ -1 & 0 & 0 & 0 \\ 0 & 0 & 0 & +1 \\ 0 & 0 & -1 & 0 \end{pmatrix},$$

respectively. Matrix columns 3 and 4 (representing a β state amide proton) add constructively, whereas columns 1 and 2 (representing an α state amide proton) have pairwise opposite signs and thus subtract. The case $\phi = -y$ follows analogously. It should again be noted that actual pulse program implementations may seemingly look different [13,14]. Furthermore, one may even deduce the kind of spectrometer used based alone on how the initial INEPT is programmed [13].

In sum, it becomes clear that a thorough theoretical understanding of spin state selective experiments and their predictable practical realization on spectrometer hardware requires precise advance knowledge of underlying phase syntax conventions.

For the reliable implementation of pulse sequences from the literature, it is thus desirable that it is clearly indicated whether phases are to be understood as spin-dynamic or, less preferably, as pulse program phases, and in the latter case, which spectrometer configuration was used. We shall remark that it would be readily possible through simple manufacturing adjustments to reconcile instrument behavior with theory, thus effectively removing any causes of confusion [7,8].

Acknowledgments

This research was supported by NIH grants GM047467 and AI037581 to G.W. and the MIT/Harvard Center for Magnetic Resonance.

References

[1] K. Pervushin, R. Riek, G. Wider, K. Wüthrich, Attenuated T_2 relaxation by mutual cancellation of dipole–dipole coupling and chemical shift anisotropy indicates an avenue to NMR structures of very large biological macromolecules in solution, Proc. Natl. Acad. Sci. USA. 94 (1997) 12366–12371.
[2] T. Parella, A complete set of novel 2D correlation NMR experiments based on heteronuclear *J*-cross polarization, J. Biomol. NMR 29 (2004) 37–55.
[3] T. Parella, Spin-state-selective excitation in gradient-selected heteronuclear cross-polarization NMR experiments, J. Magn. Reson. 167 (2004) 266–272.
[4] K.V. Pervushin, G. Wider, K. Wüthrich, Single transition-to-single transition polarization transfer (ST2-PT) in [^{15}N, ^{1}H]-TROSY, J. Biomol. NMR 12 (1998) 345–348.
[5] A. Meissner, O.W. Sørensen, Three-dimensional protein NMR TROSY-type ^{15}N-resolved $^{1}H_N$–$^{1}H_N$ NOESY spectra with diagonal peak suppression, J. Magn. Reson. 142 (2000) 195–198.
[6] M.H. Levitt, Spin Dynamics, John Wiley, Chichester, 2001.
[7] M.H. Levitt, The signs of frequencies and phases in NMR, J. Magn. Reson. 126 (1997) 164–182.
[8] M.H. Levitt, O.G. Johannessen, Signs of frequencies and phases in NMR: the role of radiofrequency mixing, J. Magn. Reson. 142 (2000) 190–194.
[9] R.R. Ernst, G. Bodenhausen, A. Wokaun, Principles of Nuclear Magnetic Resonance in One and Two Dimensions, Oxford University Press, Oxford, 1988.
[10] M. Helgstrand, P. Allard, QSim, a program for NMR simulations, J. Biomol. NMR 30 (2004) 71–80.
[11] N. Tjandra, A. Szabo, A. Bax, Protein backbone dynamics and ^{15}N chemical shift anisotropy from quantitative measurement of relaxation interference effects, J. Am. Chem. Soc. 118 (1996) 6986–6991.
[12] N. Tjandra, A. Bax, Solution NMR measurement of amide proton chemical shift anisotropy in ^{15}N-enriched proteins. Correlation with hydrogen bond length, J. Am. Chem. Soc. 119 (1997) 8076–8082.
[13] R. Konrat, D. Yang, L.E. Kay, A 4D TROSY-based pulse scheme for correlating $^{1}HN_i$, $^{15}N_i$, $^{13}C\alpha_i$, $^{13}C'_{i-1}$ chemical shifts in high molecular weight, ^{15}N, ^{13}C, ^{2}H labeled proteins, J. Biomol. NMR 15 (1999) 309–313.
[14] M. Salzmann, K. Pervushin, G. Wider, H. Senn, K. Wüthrich, TROSY in triple-resonance experiments: new perspectives for sequential NMR assignment of large proteins, Proc. Natl. Acad. Sci. USA 95 (1998) 13585–13590.